2017 IEEE International Conference on Robotics and Automation (ICRA)
Singapore, May 29 - June 3, 2017

Smooth-Path-Tracking Control of a Biped Robot at Variable Speed Based on Dynamics Morphing

Hiroshi Atsuta[1], Haruki Nozaki[2] and Tomomichi Sugihara[1]

Abstract— **This paper extends the longitudinal walking controller of biped robots proposed by one of the authors to walking along a smooth curved path. The previous controller defined in a fixed inertial frame is redesigned with respect to a moving frame attached to the center of mass (COM) of the robot in order to achieve walking along an arc. As a result, it is found that a desired position of the zero-moment point (ZMP) can be determined only from the local curvature of the referential path besides the state of the robot with respect to the moving frame. Thus, it is directly applicable to walking along an arbitrary smooth path including straight walk. In addition to the extension of the ZMP manipulation, techniques of foot control consistent with COM movement and automatic update of the referential COM position are fully extended to curved walk. The idea was examined through computer simulations to show responsiveness to updates of motion references and robustness against external disturbances.**

I. Introduction

Stable locomotion control is crucial for biped robots. In order for a biped robot to move in an unstructured environment, responsiveness to follow changes of motion command and robustness to unexpected disturbances are required.

A successful approach to biped locomotion control is to plan a sequence of footprints followed by a detailed referential trajectory [1]–[5]. The approach is effective in rather complex environments where footholds are limited. If the environment is open and regular, the preplanned footsteps and trajectory might restrict chances to stabilize against unexpected events. Instead of planning footprints in advance, recomputing where to land the foot in one or several steps has also been proposed [6]–[12]. This approach can cope with disturbances by stepping flexibly. However, it works on a hard finite state machine in each state of which the supporting foot is assumed to be firmly in contact.

On the other hand, a trajectory-free biped control has also been of interest. How to produce a self-excited oscillation for continuous stepping is important for this type of control, but in general it is difficult to design motions. In biologically-inspired approaches [13]–[15], it has difficulties to find parameters of coupled oscillators. Passive dynamic walkers [16], [17] greatly depend on the mechanisms of the robot and they are not compatible with various motions, for instance standing on site.

Sugihara [18] proposed a longitudinal locomotion control of biped robots. Although it only supposes a motion on a horizontal plane, it has several advantages; it requires no trajectory defined by time, employs an explicitly designable oscillator to produce a limit cycle for stepping and combines walking control with standing.

The goal of this paper is to extend the above controller so that it can achieve turning to other directions. Our idea is to redesign it based on a moving frame fixed to the robot. As the result, a desired position of the zero-moment point (ZMP) can be determined analytically from the local curvature of a smooth path to follow and a desired velocity along the tangential of the path. As ZMP manipulation plays roles to not only achieve a desired motion but also stabilize the motion of the center of mass (COM), it can quickly respond to updates of motion commands and external disturbances. Additionally, foot control to satisfy constraints on ZMP with avoiding interference between feet and automatic update of referential position to stop COM at the middle of the feet when reverting to standing control are also proposed.

II. Oscillation control of the center of mass along a curved path

A. Longitudinal walking based on an inertial frame [18]

Let us consider a biped robot modeled as Fig. 1, in which the total mass of the robot is concentrated at COM and it is driven by the ground reaction force. Let us denote the forward, leftward and upward directions of the robot with respect to a fixed inertial frame as x, y and z axes, respectively. Assuming that the COM height is constant, the moment about COM is small enough to be negligible and the ground reaction forces are distributed on a horizontal plane, the following equation of motion can be obtained:

$$\ddot{x} = \zeta^2(x - x_Z) \tag{1}$$

$$\ddot{y} = \zeta^2(y - y_Z), \tag{2}$$

where $\boldsymbol{p} = [x\ y\ z]^{\mathrm{T}}$, $\boldsymbol{p}_Z = [x_Z\ y_Z\ z_Z]^{\mathrm{T}}$ are positions of COM and ZMP [19], respectively, $\zeta \equiv \sqrt{g/z}$ and g is the gravitational acceleration. Eqs. (1) and (2) indicate that COM can be controlled through ZMP manipulation [20]. $\boldsymbol{p}_Z$ is constrained to lie within the convex hull of all contact points between the feet and the ground, which is represented as follows:

$$\boldsymbol{p}_Z \in \boldsymbol{S}, \tag{3}$$

*This work was supported in part by MEXT KAKENHI Grant Number JP15H02762, in part by MEXT KAKENHI Grant Number JP26540135, and in part by NEDO the International R&D and Demonstration Project in Environment and Medical Device Sector / The International R&D and Demonstration Project on Robotic Field.

[1]Hiroshi Atsuta and Tomomichi Sugihara are with Dept. of Adaptive Machine Systems, Graduate School of Engineering, Osaka University, 1-1 Yamadaoka, Suita, Osaka 565-0871, Japan hiroshi.atsuta@ams.eng.osaka-u.ac.jp, zhidao@ieee.org

[2]Haruki Nozaki is with Yamazaki Mazak Corporation, 1-131 Takeda, Oguchi-cho, Niwa-gun, Aichi 480-0147, Japan haruki.nozaki@ams.eng.osaka-u.ac.jp

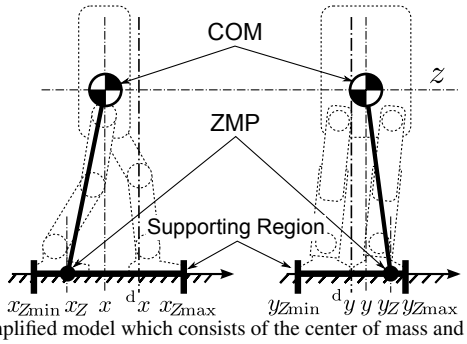

Fig. 1: Simplified model which consists of the center of mass and the ground reaction force distributed on a horizontal plane

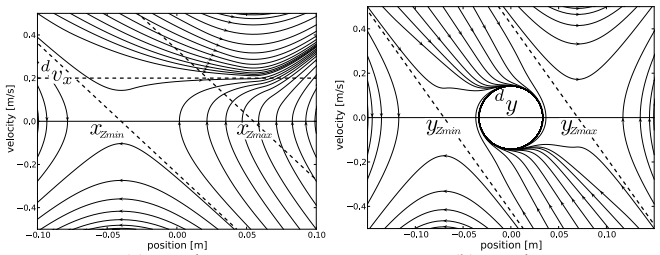

(a) x axis (b) y axis

Fig. 2: Phase portraits of the system in which (a) the controller works as a velocity follower and (b) a stable limit cycle emerges

where $\boldsymbol{S}$ is the supporting region. Notice that it discontinuously changes during motion.

A bipedal locomotion controller for walking along x axis as an autonomous system was proposed [18],

$$x_Z = x + q_x\left(x - {}^d x\right) + \frac{q_x+1}{\zeta}\left(\dot{x} - {}^d v_x\right) \tag{4}$$

$$y_Z = y + q_y\left(y - {}^d y\right) + \frac{q_y+1}{\zeta}\gamma(d)\dot{y}, \tag{5}$$

where

$$d \equiv \sqrt{(y - {}^d y)^2 + \frac{\dot{y}^2}{\zeta^2 q_y}} \tag{6}$$

$$\gamma(d) \equiv 1 - \rho \exp k\left\{1 - \frac{(q_y+1)^2 d^2}{\bar{d}^2}\right\}, \tag{7}$$

${}^d x$ and ${}^d y$ are the referential positions of COM, ${}^d v_x$ is the referential velocity of COM along x axis, $q_x(\geq 0)$, $q_y(\geq 0)$, $k(>0)$, $\bar{d}(>0)$ and $\rho(\geq 0)$ are control parameters.

Various motions can be achieved by setting the control parameters to appropriate values. When setting ${}^d v_x$ and ρ for 0, the controller (Eqs. (4)(5)) becomes the best COM-ZMP regulator [21] which stabilizes COM position to $[{}^d x\ {}^d y\ z]^{\mathrm{T}}$. When setting ρ for 1, the following stable limit cycle appears along y axis as shown in Fig. 2(b):

$$(y - {}^d y)^2 + \frac{\dot{y}^2}{\zeta^2 q_y} = \frac{\bar{d}^2}{(q_y+1)^2}, \tag{8}$$

which produces lateral oscillation for stepping [22]. q_y and $\bar{d}$ determine the period and amplitude of oscillation, respectively. When setting q_x for 0, it works as a velocity-follower shown in Fig. 2(a), which converges $\dot{x}$ to ${}^d v_x$ for walking back and forth [18].

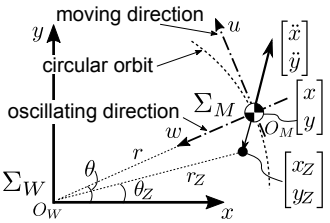

Fig. 3: The relationship between the fixed and moving frames

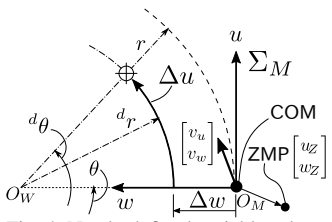

Fig. 4: Newly defined variables along the circular path

B. Coordinate transformation of the equation of motion

The previous controller cannot move the robot otherwise along x axis. To make it possible to walk in any direction, the controller should be redesigned based on a moving frame fixed to the robot.

Suppose the robot walks along an arc centered at the origin of the fixed inertial frame Σ_W as shown in Fig. 3. Note that the center of the arc can be defined anywhere without loss of generality. The COM $[x\ y]^{\mathrm{T}}$ and ZMP $[x_Z\ y_Z]^{\mathrm{T}}$ with respect to Σ_W, which are projected on the plane, can be described with respect to the polar coordinate system as follows:

$$\begin{bmatrix} x \\ y \end{bmatrix} = r\begin{bmatrix} \cos\theta \\ \sin\theta \end{bmatrix} \qquad \begin{bmatrix} x_Z \\ y_Z \end{bmatrix} = r_Z\begin{bmatrix} \cos\theta_Z \\ \sin\theta_Z \end{bmatrix}, \tag{9}$$

where (r, θ) and (r_Z, θ_Z) are the polar coordinates for COM and ZMP, respectively.

Differentiating Eq. (9) with respect to time gives the velocity and acceleration of COM,

$$\begin{bmatrix} \dot{x} \\ \dot{y} \end{bmatrix} = \dot{r}\begin{bmatrix} \cos\theta \\ \sin\theta \end{bmatrix} + r\dot{\theta}\begin{bmatrix} -\sin\theta \\ \cos\theta \end{bmatrix} \tag{10}$$

$$\begin{bmatrix} \ddot{x} \\ \ddot{y} \end{bmatrix} = (\ddot{r} - r\dot{\theta}^2)\begin{bmatrix} \cos\theta \\ \sin\theta \end{bmatrix} + (2\dot{r}\dot{\theta} + r\ddot{\theta})\begin{bmatrix} -\sin\theta \\ \cos\theta \end{bmatrix}. \tag{11}$$

By substituting Eqs. (9)(11) into Eqs. (1)(2), we obtain the following equation of motion,

$$(\ddot{r} - r\dot{\theta}^2)\begin{bmatrix} \cos\theta \\ \sin\theta \end{bmatrix} + (2\dot{r}\dot{\theta} + r\ddot{\theta})\begin{bmatrix} -\sin\theta \\ \cos\theta \end{bmatrix} = \zeta^2\left(r\begin{bmatrix} \cos\theta \\ \sin\theta \end{bmatrix} - r_Z\begin{bmatrix} \cos\theta_Z \\ \sin\theta_Z \end{bmatrix}\right). \tag{12}$$

Let us consider a new coordinate system Σ_M whose origin is located on the position of COM of the robot, and the tangential direction, u axis, and the radial direction, w axis, correspond to the forward and leftward directions of the robot, respectively (Fig. 3). The relationship between an arbitrary point with respect to Σ_W $[X\ Y]^{\mathrm{T}}$ and its correspondent coordinates with respect to Σ_M $[u\ w]$ is expressed as follows:

$$\begin{bmatrix} X \\ Y \end{bmatrix} = \begin{bmatrix} x \\ y \end{bmatrix} + \begin{bmatrix} -\sin\theta & -\cos\theta \\ \cos\theta & -\sin\theta \end{bmatrix}\begin{bmatrix} u \\ w \end{bmatrix}$$
$$\Leftrightarrow \begin{bmatrix} u \\ w \end{bmatrix} = \begin{bmatrix} -\sin\theta & \cos\theta \\ -\cos\theta & -\sin\theta \end{bmatrix}\begin{bmatrix} X - x \\ Y - y \end{bmatrix}. \tag{13}$$

Eq. (12) turns to the following equation:

$$2\dot{r}\dot{\theta} + r\ddot{\theta} = \zeta^2 r_Z \sin(\theta - \theta_Z) \tag{14}$$

$$-\ddot{r} + r\dot{\theta}^2 = -\zeta^2\{r - r_Z\cos(\theta - \theta_Z)\}. \tag{15}$$

Let the ZMP position with respect to Σ_M be denoted as $[u_Z\ w_Z]^{\mathrm{T}}$, then we get the following from Eqs. (9) and (13),

$$\begin{bmatrix} x_Z \\ y_Z \end{bmatrix} = \begin{bmatrix} x \\ y \end{bmatrix} + \begin{bmatrix} -\sin\theta & -\cos\theta \\ \cos\theta & -\sin\theta \end{bmatrix} \begin{bmatrix} u_Z \\ w_Z \end{bmatrix}$$
$$\Leftrightarrow \begin{bmatrix} u_Z \\ w_Z \end{bmatrix} = \begin{bmatrix} -r_Z \sin(\theta - \theta_Z) \\ r - r_Z \cos(\theta - \theta_Z) \end{bmatrix}. \quad (16)$$

Substituting Eq. (16) into Eqs. (14)(15) gives the equation of motion with respect to Σ_M,

$$2\dot{r}\dot{\theta} + r\ddot{\theta} = -\zeta^2 u_Z, \quad (17)$$
$$-\ddot{r} + r\dot{\theta}^2 = -\zeta^2 w_Z. \quad (18)$$

The terms $r\dot{\theta}^2$ and $2\dot{r}\dot{\theta}$ are equivalent to accelerations due to centrifugal force and Coriolis force, respectively.

C. Redesign of the controller based on a moving frame

As u_Z and w_Z in Eqs. (17)(18) are considered as a control input, we redesign a new controller with respect to Σ_M in a similar way to the previous controller Eqs. (4)(5) as follows:

$$u_Z = q_u r(\theta - {}^d\theta) + \frac{q_u + 1}{\zeta} r(\dot{\theta} - {}^d\omega) + \frac{2\dot{r}\dot{\theta}}{\zeta^2} \quad (19)$$

$$w_Z = -q_w(r - {}^d r) - \frac{q_w + 1}{\zeta}\gamma(d)\dot{r} - \frac{r\dot{\theta}^2}{\zeta^2}, \quad (20)$$

where

$$d \equiv \sqrt{(r - {}^d r)^2 + \frac{\dot{r}^2}{\zeta^2 q_w}}, \quad (21)$$

$$\gamma(d) \equiv 1 - \rho \exp k\left(1 - \frac{(q_w + 1)^2 d^2}{\bar{d}^2}\right), \quad (22)$$

q_u, q_w, k, $\bar{d}$ and ρ are non-negative control parameters, ${}^d\theta$ and ${}^d\omega$ are the referential angle and the angular velocity centered at the origin of Σ_M, respectively, and ${}^d r$ is the radius of the referential circular path. As in the case of x-y coordinate system, the nonlinear term $\gamma(d)$ has an effect to make a self-excited oscillation of COM along w axis appear.

It should be noticed that Eqs. (19)(20) are coupled with each other while the previous controllers were decoupled, and centrifugal and Colioris forces can be compensated.

θ, $\dot{\theta}$, r and $\dot{r}$ in Eqs. (19)(20) are global information of the motion, which means that these variables are measured with respect to the world frame Σ_W. It is difficult for the robot to observe them. For the same reason, providing ${}^d\theta$, ${}^d\omega$ and ${}^d r$ as references of motion is not suited for mobile robots that move freely.

Suppose we have an arc which is concentric with the referential circular path and crosses COM as shown in Fig. 4. We define two new variables; $\Delta w = r - {}^d r$, the displacement between COM position and the referential path along the radial direction, and $\Delta u = {}^d r({}^d\theta - \theta)$, the arc length to the referential position along the referential path.

Assuming COM has a velocity $[\dot{x}\ \dot{y}]^{\mathrm{T}}$ with respect to Σ_W leads the following relationship:

$$\begin{bmatrix} v_u \\ v_w \end{bmatrix} = \begin{bmatrix} -\sin\theta & \cos\theta \\ -\cos\theta & -\sin\theta \end{bmatrix} \begin{bmatrix} \dot{x} \\ \dot{y} \end{bmatrix} = \begin{bmatrix} r\dot{\theta} \\ -\dot{r} \end{bmatrix}, \quad (23)$$

where $[v_u\ v_w]^{\mathrm{T}}$ is the velocity of COM with respect to Σ_M. The referential velocity ${}^d v_u$ along u axis can be denoted as ${}^d v_u = {}^d r\,{}^d\omega$, and by substituting these relationships into Eqs. (19)(20)(21) we obtain a new control input,

$$u_Z = -q_u \frac{{}^d r + \Delta w}{{}^d r}\Delta u + \frac{q_u + 1}{\zeta}\left(v_u - \frac{{}^d r + \Delta w}{{}^d r}{}^d v_u\right) + \frac{2 v_u v_w}{\zeta^2({}^d r + \Delta w)} \quad (24)$$

$$w_Z = q_w \Delta w + \frac{q_w + 1}{\zeta}\gamma(d) v_w - \frac{v_u^2}{\zeta^2({}^d r + \Delta w)} \quad (25)$$

$$d \equiv \sqrt{\Delta w^2 + \frac{v_w^2}{\zeta^2 q_w}}. \quad (26)$$

Though Eqs. (24)(25) are mathematically correct, there is a problem when implementing them on a computer. The straight walking is achieved by setting ${}^d r$ to ∞, which unfits to the digital representation, so it has to be distinguished from curved walking. Let us introduce curvature of the referential path, $\kappa = \frac{1}{{}^d r}$, which gives the following relationship:

$$r = {}^d r + \Delta w \quad \Leftrightarrow \quad \frac{{}^d r + \Delta w}{{}^d r} = 1 + \kappa \Delta w. \quad (27)$$

Thus, Eqs. (24)(25) are reduced to the following:

$$u_Z = -q_u(1 + \kappa\Delta w)\Delta u + \frac{q_u + 1}{\zeta}\{v_u - (1 + \kappa\Delta w)^d v_u\} + \frac{2\kappa v_u v_w}{\zeta^2(1 + \kappa\Delta w)} \quad (28)$$

$$w_Z = -q_w \Delta w + \frac{q_w + 1}{\zeta}\gamma(d) v_w - \frac{\kappa v_u^2}{\zeta^2(1 + \kappa\Delta w)}. \quad (29)$$

When $\kappa = 0$, Eqs. (28)(29) become

$$u_Z = -q_u \Delta u + \frac{q_u + 1}{\zeta}\{v_u - {}^d v_u\} \quad (30)$$

$$w_Z = -q_w \Delta w + \frac{q_w + 1}{\zeta}\gamma(d) v_w. \quad (31)$$

Eqs. (30)(31) show that they are equivalent to the straight walking controller Eqs. (4)(5).

The controller has some advantageous features: (i) The referential path can be given as an arbitrary smooth curve since a parameter to represent the path is only the curvature, κ, at the position of the robot. (ii) The motion references, ${}^d v_u$ and κ, can be given from the first-person view of the robot, which is favorable for applications to remote operation of robots. (iii) The states, Δu, Δw, v_u and v_w, can be observed from the egocentric frame of reference of the robot.

III. Consistent foot control and automatic update of referential position

A. Consistent foot control with COM movement

In our control scheme, the desired ZMP position can be determined just from the local motion references and the current state of COM, which means that neither a sequence of footprints nor a trajectory of ZMP are required. In order for the robot to walk endlessly, however, the supporting region has to be deformed so as to satisfy Eq. (3) consistently with

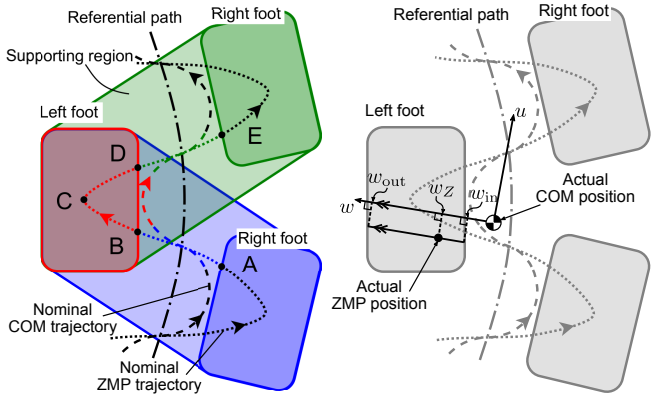

(a) Nominal COM and ZMP trajectories: ZMP passes in alphabetical order in the figure

(b) The relative position of the actual ZMP between the inner and outer edges of the sole

Fig. 5: Nominal trajectories of COM and ZMP and a sequence of footsteps

COM movement. There are two key points to achieve the consistent foot control; when to lift off and touch on the ground and where to place the foot.

First, the foot-lifting control for straight walking [18] will be extended to curved walking, where the feet does not face toward the moving direction. We have to know when ZMP comes into (the point B in Fig. 5(a)) and goes out (the point D in the same figure) of the supporting foot. Although the directions of the soles coincide with the axes of the coordinate system in straight walking, the assumption is not always accepted in curved walking. Fig. 5(b) shows how to find out the relative position of the actual ZMP between the inner and outer edges of the sole. Let us define a complex number c_Z to map the motion of COM and ZMP as follows:

$$c_Z = w_Z - \Delta w - \frac{(q_w+1)\,v_w}{\zeta\sqrt{q_w}}\,i. \tag{32}$$

The coefficient of the imaginary part is chosen so that c_Z draws a circle on the complex plane as shown in Fig. 6. The points B and D in Fig. 5(a) correspond to $\bar{c}_0$ and $\bar{c}_1$ on the complex plane, respectively, which are obtained as follows:

$$\bar{c}_0 = w_{\text{in}} - \Delta w - \sqrt{|c_Z|^2 - (w_{\text{in}} - \Delta w)^2}\,i \tag{33}$$

$$\bar{c}_1 = w_{\text{in}} - \Delta w + \sqrt{|c_Z|^2 - (w_{\text{in}} - \Delta w)^2}\,i. \tag{34}$$

A phase ϕ which represents the relative position of c_Z between $\bar{c}_0$ and $\bar{c}_1$ can be defined as follows:

$$\phi \equiv \angle\frac{(c_Z/\bar{c}_0)}{(\bar{c}_1/\bar{c}_0)}. \tag{35}$$

ϕ changes 0 to 1 monotonically during the single support phase. The desired lifting height of the foot is defined as

$${}^d z_{KF} = \frac{1}{2}\frac{h_{\max}|c_Z|}{\bar{d}}\left(1-\cos 2\pi\phi\right), \tag{36}$$

where $h_{\max}$ is maximum height of foot.

Next, the foot placement decision will be described. In the previous work [18], the desired landing position of the kicking foot is determined by the strong standing-stabilizability condition proposed by Sugihara [21]. This idea is similar to the (instantaneous) capture point [23], [24], but the difference is that the former takes into account the property of the controller. We can get a point that meets the strong standing-stabilizability condition by transformation of Σ_W to Σ_M:

$$u_{SP} = \frac{q_u+1}{\zeta}v_u - q_u\,(1+\kappa\Delta w)\,\Delta u + \frac{2\kappa v_u v_w}{\zeta^2\,(1+\kappa\Delta w)} \tag{37}$$

$$w_{SP} = \frac{q_w+1}{\zeta}v_w - q_w\Delta w - \frac{\kappa v_u^2}{\zeta^2\,(1+\kappa\Delta w)}. \tag{38}$$

In the previous control, the collision between the feet did not need to be taken into account since the foot moves in a straight line. However, as the robot walks along a curved path, the kicking foot might collide with the supporting foot. Let us consider two concentric arcs that pass the feet as shown in Fig. 7. Imposing a constraint on desired landing foot position so as not to place between the arcs avoids the collision. Hence, the desired landing position of the kicking foot is represented as follows:

$$\begin{bmatrix} {}^d u_{KF} \\ {}^d w_{KF} \end{bmatrix} = \begin{bmatrix} u_{SP} \\ w_{SP} \end{bmatrix} + \Delta r_{KF}\begin{bmatrix} -\sin\varphi_{KF} \\ \cos\varphi_{KF} \end{bmatrix}, \tag{39}$$

where

$$\tan\varphi_{KF} = \frac{\kappa u_{SP}}{1+\kappa\Delta w - \kappa w_{SP}} \tag{40}$$

$$\Delta w_{SP} = u_{SP}\tan\frac{\varphi_{KF}}{2} + \Delta w - w_{SP} \tag{41}$$

$$\Delta r_{KF} = \bar{d} - \Delta w_{SP}. \tag{42}$$

φ_{KF}, Δw_{SP} and Δr_{KF} are indicated in Fig. 7, which are obtained from geometric relationships shown in Appendix.

B. Automatic update of referential COM position

As pointed out in [18], the referential position along moving direction, ${}^d x$ in Eq. (4), disappears in the velocity following control, namely $q_x = 0$. If ${}^d x$ at the start of moving remains, the robot may lose balance when getting back to standing. In [18], ${}^d x$ was always updated by the the current position and ${}^d y$ was constant. In curved walk, as controllers for u and w axes are coupled with each other, the referential position has to be updated along the referential curved path.

Let us denote the desired COM position after Δt seconds as $[u'\ w']$, we can obtain the following relationships in the same way as Eqs. (40)(41) (see Appendix),

$$\tan\varphi' = \frac{\kappa u'}{1+\kappa\Delta w - \kappa w'} \tag{43}$$

$$\Delta w' = u'\tan\frac{\varphi'}{2} + \Delta w - w'. \tag{44}$$

Therefore, a referential position of COM after Δt seconds $[{}^d u'\ {}^d w']$ can be obtained as

$$\begin{bmatrix} {}^d u' \\ {}^d w' \end{bmatrix} = \begin{bmatrix} u' \\ w' \end{bmatrix} + \Delta w'\begin{bmatrix} -\sin\varphi' \\ \cos\varphi' \end{bmatrix}. \tag{45}$$

It should be noted that $\Delta w'$ is an expected state along w axis after Δt seconds.

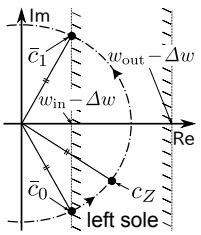

Fig. 6: Trajectory of c_Z when ZMP comes into and goes out of the sole

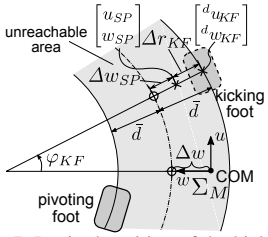

Fig. 7: Desired position of the kicking foot to avoid a collision

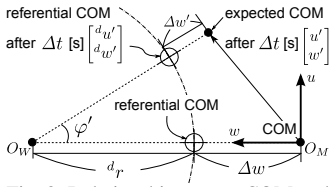

Fig. 8: Relationship among COM and its referential positions

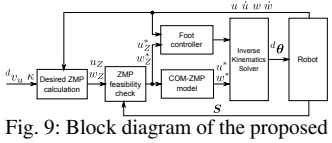

Fig. 9: Block diagram of the proposed control scheme

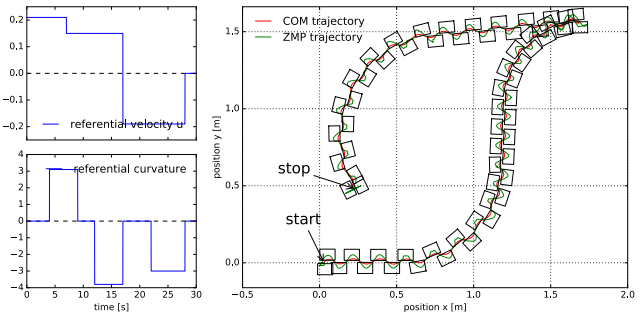

Fig. 10: Result of simulation A

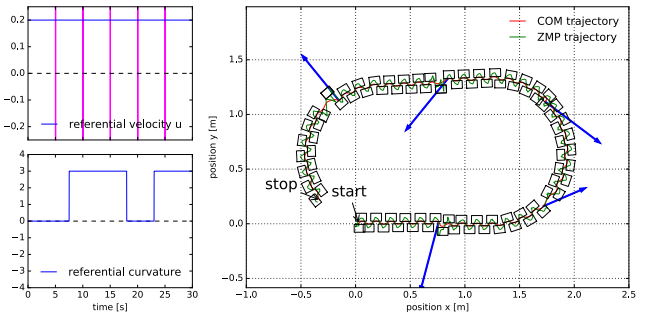

(a) Trajectories of COM and ZMP and footprints

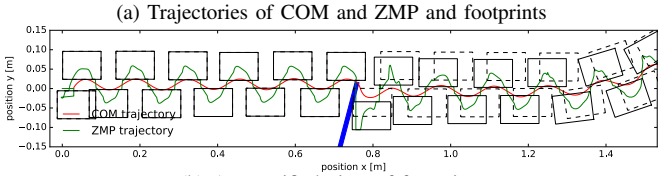

(b) A magnified view of footprints

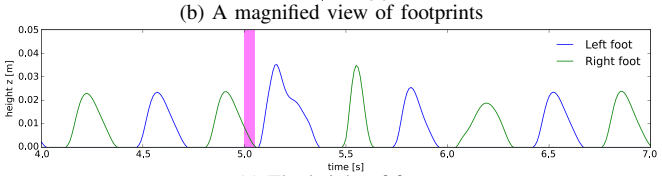

(c) The height of feet

Fig. 11: Result of simulation B

IV. Simulations and Discussion

A. Simulations

Simulations was executed to validate the proposed controller. An anthropomorphic robot "mighty" [25] was supposed. The desired ZMP was replaced by the nearest point of $\boldsymbol{S}$ if it is not within $\boldsymbol{S}$. The joint displacements of the whole body were obtained by solving inverse kinematics from the desired COM and feet positions. Fig. 9 shows the structure of our control scheme. The control parameters are set to $z = 0.26$[m], $q_u = 0.5$, $k = 1$ and $h_{max} = 0.02$[m].

Simulation A was conducted to make sure that motion commands can be changed during motion. Motion commands, ${}^d v_u$ and κ, were modified at random during the simulation. Fig. 10 shows a sequence of footprints and trajectories of actual COM and ZMP. The robot could walk freely and stop without falling.

Simulation B was conducted to make sure that the robot can stabilize against external forces. Random magnitudes and directions of forces were applied to COM every 5 seconds. Fig. 11(a) shows trajectories of actual COM and ZMP, footprints and forces indicated by blue arrows. As it can be observed, the robot could respond to external disturbances by stepping out the foot. Fig. 11(b) shows a magnified view of footprints when the robot is subjected to the first force. Dotted lines are footprints if the force were not applied. Compared with them, the robot could respond to unknown disturbances by stepping. Fig. 11(c) shows height of feet around when the first force is applied. The timings to lift off and touch on the foot are flexibly modified.

B. Discussion

To apply the proposed controller to a real robot, we have some issues. First, in our control scheme, the actual ZMP is assumed to follow the desired ZMP. However, as ZMP cannot be moved directly, we have to manipulate it through the whole body motion. How to compensate the errors is out of the range of this paper, but introducing an external force observer could be considered. Second, to feedback the current state of the robot an estimation of COM is required. The estimation of COM is generally a difficult problem, but a slight amount of errors can be handled same as external forces. It should be evaluated how much amount of errors can be allowed. Third, the controller assumed the surface was open and flat. It is not suited for environments where footholds are limited. However, on uneven terrain which has small bumps like gravelly road, the fluctuation can also be handled as external disturbances. We should investigate the stability on those surface.

V. Conclusion

A novel biped controller which can follow an arbitrary smooth curved path is proposed based on the dynamics morphing. Although the previous controller was fixed on the world frame, by transformation of it with respect to a moving frame attached to the robot turning to other directions was

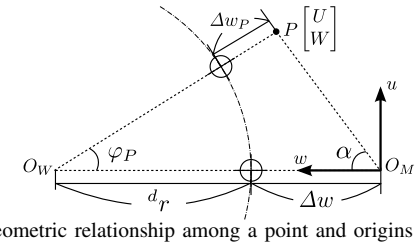

Fig. 12: Geometric relationship among a point and origins of the frames

achieved. Consistent foot control with movement of COM and automatic update of referential position for issuing stop command at any time were also proposed. The validity of our controller was examined through computer simulations.

APPENDIX

Fig. 12 shows a geometric relationship among a point w.r.t Σ_M and the origins of the two coordinate systems. Let us represent Δw_P with Δw, κ, U and W.

The angle α has the following relationships:

$$\sin\alpha = \frac{U}{\sqrt{U^2+W^2}}, \quad \cos\alpha = \frac{W}{\sqrt{U^2+W^2}}. \tag{46}$$

Using the law of sines for $\triangle PO_W O_M$,

$$\frac{\sqrt{U^2+W^2}}{\sin\varphi_P} = \frac{{}^d r + \Delta w}{\sin(\varphi_P+\alpha)}. \tag{47}$$

We can get the following equation from Eq. (46),

$$\sin(\varphi_P+\alpha) = \frac{1}{\sqrt{U^2+W^2}}\left(U\cos\varphi_P + W\sin\varphi_P\right). \tag{48}$$

Eqs. (47)(48) provide the relationship between φ_P and κ,

$$\tan\varphi_P = \frac{U}{{}^d r + \Delta w - W} = \frac{\kappa U}{1+\kappa\Delta w - \kappa W}, \tag{49}$$

$$\frac{1}{\kappa} = \frac{U}{\tan\varphi_P} - (\Delta w - W). \tag{50}$$

And we can get Δw_P

$$\begin{aligned} U &= \left({}^d r + \Delta w_P\right)\sin\varphi_P \\ \Leftrightarrow \Delta w_P &= \frac{U}{\sin\varphi_P} - \frac{1}{\kappa} = \frac{U}{\sin\varphi_P} - \frac{U}{\tan\varphi_P} + (\Delta w - W) \\ &= U\tan\frac{\varphi_P}{2} + \Delta w - W. \end{aligned} \tag{51}$$

REFERENCES

[1] S. Kuindersma, R. Deits, M. Fallon, A. Valenzuela, H. Dai, F. Permenter, T. Koolen, P. Marion, and R. Tedrake, "Optimization-based locomotion planning, estimation, and control design for the atlas humanoid robot," *Autonomous Robots*, vol. 40, no. 3, pp. 429–455, 2016.

[2] J. Englsberger, C. Ott, and A. Albu-Schaffer, "Three-Dimensional Bipedal Walking Control Based on Divergent Component of Motion," *IEEE Transactions on Robotics*, vol. 31, no. 2, pp. 355–368, 2015.

[3] M. A. Hopkins, D. W. Hong, and A. Leonessa, "Humanoid locomotion on uneven terrain using the time-varying divergent component of motion," in *2014 IEEE-RAS International Conference on Humanoid Robots*, 2014, pp. 266–272.

[4] S. Song, Y.-J. Ryoo, and D. W. Hong, "Development of an Omnidirectional Walking Engine for Full-Sized Lightweight Humanoid Robots," in *Volume 6: 35th Mechanisms and Robotics Conference, Parts A and B*, 2011, pp. 847–854.

[5] J. E. Chestnutt, M. Lau, G. Cheung, J. Kuffner, J. Hodgins, and T. Kanade, "Footstep Planning for the Honda ASIMO Humanoid," in *Proceedings of the 2005 IEEE International Conference on Robotics and Automation*, 2005, pp. 629–634.

[6] S. Kajita, M. Morisawa, K. Harada, K. Kaneko, F. Kanehiro, K. Fujiwara, and H. Hirukawa, "Biped Walking Pattern Generator allowing Auxiliary ZMP Control," in *Proceedings of the 2006 IEEE/RSJ International Conference on Intelligent Robots and Systems*, vol. 2, 2006, pp. 2993–2999.

[7] P.-B. Wieber, "Trajectory Free Linear Model Predictive Control for Stable Walking in the Presence of Strong Perturbations," in *Proceedings of the 2006 IEEE-RAS International Conference on Humanoid Robots*, 2006, pp. 137–142.

[8] K. Nishiwaki and S. Kagami, "Online Walking Control System for Humanoids with Short Cycle Pattern Generation," *The International Journal of Robotics Research*, vol. 28, no. 6, pp. 729–742, 2009.

[9] A. Herdt, N. Perrin, and P.-B. Wieber, "Walking without thinking about it," in *Proceedings of the 2010 IEEE/RSJ International Conference on Intelligent Robots and Systems*, 2010, pp. 190–195.

[10] D. Dimitrov, A. Paolillo, and P.-B. Wieber, "Walking motion generation with online foot position adaptation based on ℓ_1- and ℓ_∞-norm penalty formulations," in *2011 IEEE International Conference on Robotics and Automation*, 2011, pp. 3523–3529.

[11] M. Missura and S. Behnke, "Omnidirectional capture steps for bipedal walking," in *Proceedings of the 2013 IEEE-RAS International Conference on Humanoid Robots*, 2013, pp. 14–20.

[12] R. J. Griffin and A. Leonessa, "Model predictive control for dynamic footstep adjustment using the divergent component of motion," in *2016 IEEE International Conference on Robotics and Automation (ICRA)*, 2016, pp. 1763–1768.

[13] R. Katoh and M. Mori, "Control method of biped locomotion giving asymptotic stability of trajectory," *Automatica*, vol. 20, no. 4, pp. 405–414, 1984.

[14] G. Taga, Y. Yamaguchi, and H. Shimizu, "Self-organized control of bipedal locomotion by neural oscillators in unpredictable environment," *Biological Cybernetics*, vol. 65, no. 3, pp. 147–159, 1991.

[15] J. Morimoto, G. Endo, J. Nakanishi, and G. Cheng, "A Biologically Inspired Biped Locomotion Strategy for Humanoid Robots: Modulation of Sinusoidal Patterns by a Coupled Oscillator Model," *IEEE Transactions on Robotics*, vol. 24, no. 1, pp. 185–191, 2008.

[16] T. McGeer, "Passive Dynamic Walking," *The International Journal of Robotics Research*, vol. 9, no. 2, pp. 62–82, 1990.

[17] S. H. Collins, M. Wisse, and A. Ruina, "A Three-Dimensional Passive-Dynamic Walking Robot with Two Legs and Knees," *The International Journal of Robotics Research*, vol. 20, no. 7, pp. 607–615, 2001.

[18] T. Sugihara, "Biped control to follow arbitrary referential longitudinal velocity based on dynamics morphing," in *Proceedings of the 2012 IEEE/RSJ International Conference on Intelligent Robots and Systems*, 2012, pp. 1892–1897.

[19] M. Vukobratović and J. Stepanenko, "On the stability of anthropomorphic systems," *Mathematical Biosciences*, vol. 15, no. 1-2, pp. 1–37, 1972.

[20] K. Mitobe, G. Capi, and Y. Nasu, "Control of walking robots based on manipulation of the zero moment point," *Robotica*, vol. 18, pp. 651–657, 2000.

[21] T. Sugihara, "Standing stabilizability and stepping maneuver in planar bipedalism based on the best COM-ZMP regulator," in *Proceedings of the 2009 IEEE International Conference on Robotics and Automation*, 2009, pp. 1966–1971.

[22] ——, "Consistent biped step control with COM-ZMP oscillation based on successive phase estimation in dynamics morphing," in *Proceedings of the 2010 IEEE International Conference on Robotics and Automation*, 2010, pp. 4224–4229.

[23] J. Pratt, J. Carff, S. Drakunov, and A. Goswami, "Capture Point: A Step toward Humanoid Push Recovery," in *Proceedings of the 2006 IEEE-RAS International Conference on Humanoid Robots*, 2006, pp. 200–207.

[24] T. Koolen, T. de Boer, J. Rebula, A. Goswami, and J. Pratt, "Capturability-based analysis and control of legged locomotion, Part 1: Theory and application to three simple gait models," *The International Journal of Robotics Research*, vol. 31, no. 9, pp. 1094–1113, 2012.

[25] T. Sugihara, K. Yamamoto, and Y. Nakamura, "Hardware design of high performance miniature anthropomorphic robots," *Robotics and Autonomous Systems*, vol. 56, no. 1, pp. 82–94, 2008.